ANALYSIS OF THE TIME-VARYING CORTICAL NEURAL CONNECTIVITY IN THE NEWBORN EEG: A TIME-FREQUENCY APPROACH

Amir Omidvarnia, Mostefa Mesbah, John M. O'Toole, Paul Colditz, Boualem Boashash

The University of Queensland, UQ Centre for Clinical Research, QLD 4029, Australia

ABSTRACT

Relationships between cortical neural recordings as a representation of functional connectivity between cortical brain regions were quantified using different time-frequency criteria. Among these, Partial Directed Coherence (PDC) and Directed Transfer Function (DTF) and their extensions have found wide acceptance. This paper aims to assess and compare the performance of these two connectivity measures that are based on time-varying multivariate AR modeling. The time-varying parameters of the AR model are estimated using an Adaptive AR modeling (AAR) approach and a short-time based stationary approach. The performance of these two approaches is compared using both simulated signal and a multichannel newborn EEG recording. The results show that the time-varying PDC outperforms the time-varying DTF measure. The results also point to the limitation of the AAR algorithm in tracking rapid parameter changes and the drawback of the short-time approach in providing high resolution time-frequency coherence functions. However, it can be demonstrated that time-varying MVAR representations of the cortical connectivity will potentially lead to better understanding of non-symmetric relations between EEG channels.

1. MEDICAL PROBLEM AND SIGNAL PROCESSING FORMULATION: BACKGROUND AND REVIEW

The ability of the brain to conduct high level sensory and cognitive functions depends strongly on underlying interactions between different brain regions [1]. Insights into the inter-relations across the brain provide a basis for understanding high level mechanisms of both healthy and pathological brain function. Scalp EEG recordings are projections of deep brain and cortical activity and can be considered as the manifestations of the brain sources at the scalp level. Despite some more accurate methods for investigating neural interrelations in the brain such as fMRI or ECoG, in many cases scalp EEG studies are preferred due to their non-invasive nature and low cost.

Multivariate autoregressive (MVAR) models are able to represent interactions between EEG signals in the form of linear difference equations [2, 3]. The general form of the time-varying MVAR models is presented in section 2.2. By using the multivariate AR representation of EEG signals, not only can the direction of the information flow between channels be inferred, but also the direct or indirect influences detected. Directed Coherence [4, 5], Partial Directed Coherence (PDC) [5], Generalized Partial Directed Coherence (GPDC) [6], Directed Transfer Function (DTF) [3], direct Directed Transfer Function (dDTF) [7] and Granger Causality Index (GCI) [8] are MVAR-based criteria which have been introduced to determine directional influence in multivariate systems. Except for GCI, which is a time-domain measure, the other criteria are frequency-based.

The assumption on which all these methods are based is that the underlying signals are stationary and that their interactions are constant over time. In other words, all of them assume time-invariant MVAR parameters. However, EEG signals are non-stationary [9]. Moreover, the mutual influence of brain regions and, therefore, of EEG channels doesn't necessarily show a time-invariant behavior. Therefore, new time dependant forms of the connectivity measures need to be introduced in such non-stationary signal analysis applications.

A number of solutions have been suggested to account for the problem of time-varying directional interactions between EEG channels. In [10], the authors used the idea of short-time DTF (ST-DTF) to divide the entire data into short overlapping time intervals and to compute the DTF measure for each interval and plot a time-frequency map of the information flow for each pair of channels. In another approach, model parameters of a time-varying MVAR are estimated by using adaptive methods such as Recursive Least-Squared or Kalman filtering and then a parametric time-frequency map, including functional relationships between channels, is produced using the estimated parameters [11, 12]. Analysis results of the above-mentioned studies on both simulated and real EEG signals suggest that the MVAR parameter estimation approaches based on Kalman filtering and its extensions are good candidates for non-stationary signal analysis [12-14]. Extended versions of Kalman filter-based estimators are capable of simultaneous modeling of nonlinearity and rapid time-varying behavior of the signals. In this paper, the suitability of an adaptive AR model algorithm based on Kalman filtering for newborn EEG signal analysis is investigated and compared with the short-time based approach. Ability of tracking fast parameter changes as well as the image resolution of the time-frequency representations are two important criteria which have been taken into consideration in this

978-1-4577-0690-5/11/$26.00 ©2017 IEEE

comparative study. The AAR algorithm has previously been used for other applications such as brain-computer interface (BCI) systems [13].

The paper is organized as follows. Section 2 describes the data used as well as the time-varying PDC and DTF measures based on an adaptive AR modeling approach and the windowing (short-time) approach. In section 3, the results of these two methods on the simulated and newborn EEG data that includes a seizure are presented. Section 4 concludes the paper.

2. METHODS

First, we used the ARFIT algorithm to fix an optimum model order for the time-varying MVAR model. ARFIT package estimates both the time-invariant parameters of the MVAR model and its optimum order [15]. The order estimation uses Schwarz's Bayesian Criterion (SBC) [16]. The estimated model order (p_{opt}) was then fixed for the remainder of the analysis. Time-varying PDCs and DTFs were computed based on the time-varying MVAR model fitted to the signal using an Adaptive AR modeling (AAR) algorithm. This algorithm uses Kalman filtering [13] for parameter estimation. A surrogate data method with 50 realizations was then used to select the most significant values of the measures at 99% confidence level. Surrogates were obtained by randomizing all samples of the signal to remove all causal relationships between them [17]. In the following, the measures, the Kalman filter-based AAR algorithm and the short-time approach are briefly introduced.

2.1. Time-varying MVAR parameter estimation using the linear Kalman filtering

The AAR algorithm based on Kalman filtering has successfully been used for the analysis of physiological signals [13, 14]. The question addressed here is whether it is suitable for newborn EEG analysis as well. The algorithm adopts the linear Kalman filtering approach to update the MVAR parameters for each time sample. To this end, MVAR equations are reformulated in the form of state space equations by re-arranging all matrix parameters into a state vector of the dynamical system and considering the non-stationary signal as the observation; that is:

$$\begin{cases} \boldsymbol{a}(n) = \boldsymbol{a}(n-1) + K(n)e(n) \\ \hat{x}(n) = C(n)\boldsymbol{a}(n) \end{cases} \quad (1)$$

where $\boldsymbol{a}(n)$ is the parameters vector (state vector), $K(n)$ is the Kalman gain, $C(n)$ is the measurement matrix, $e(n)$ is the one-step prediction error and $\hat{x}(n)$ is the estimated vector. $\boldsymbol{a}(n)$ and $C(n)$ can be represented as follows:

$$\boldsymbol{a}(n) = \begin{bmatrix} a_{11}(1,n) \\ \vdots \\ a_{1M}(p,n) \\ \vdots \\ a_{M1}(1,n) \\ \vdots \\ a_{MM}(p,n) \end{bmatrix} \quad (2)$$

$$C(n) = \begin{bmatrix} \boldsymbol{x}^T(n-1) & \cdots & 0 \\ \vdots & \ddots & \vdots \\ 0 & \cdots & \boldsymbol{x}^T(n-1) \end{bmatrix} \quad (3)$$

where $\boldsymbol{x}^T(n-1) = [x^T(n-1) \ \ldots \ x^T(n-p)]$. The elements of the state vector $\boldsymbol{a}(n)$ are estimated by using classical Kalman filtering approach. Process and observation noise covariance matrices ($W(n)$ and $V(n)$, respectively) can be updated by different methods [13, 18]. For this study, the following update equations and the update coefficient (UC) of 0.0001 led to the best performance.

$$V(n) = (1 - UC) \times V(n-1) + UC \times e(n) \quad (4)$$

$$W(n) = I \times UC \times trace(Z(n))/p \quad (5)$$

where $Z(n)$ is the a-posteriori correlation matrix, I is the identity matrix, p is the model order and '×' shows the matrix product operator. The speed of adaptation, the time resolution and the smoothing of the AR estimates are determined by the parameter UC [13].

2.2. Adaptive connectivity measures

A time-varying N-variate AR process of order p can be represented as:

$$\begin{bmatrix} x_1(n) \\ \vdots \\ x_N(n) \end{bmatrix} = \sum_{r=1}^{p} \boldsymbol{A}_r(n) \begin{bmatrix} x_1(n-r) \\ \vdots \\ x_N(n-r) \end{bmatrix} + \begin{bmatrix} w_1(n) \\ \vdots \\ w_N(n) \end{bmatrix} \quad (6)$$

where $\boldsymbol{w}$ is a vector white noise, the matrices $\boldsymbol{A}_r$ are given by:

$$\boldsymbol{A}_r(n) = \begin{bmatrix} a_{11}(r,n) & \cdots & a_{1N}(r,n) \\ \vdots & \ddots & \vdots \\ a_{N1}(r,n) & \cdots & a_{NN}(r,n) \end{bmatrix} \quad (7)$$

for $r = 1, \ldots, p$ and their elements are estimated using the adaptive approach described in section 2.1. A number of time-varying connectivity measures can be defined based on the following transformation of the MVAR parameters ($\boldsymbol{A}_r(n)$) to the frequency domain:

$$\boldsymbol{A}(n,f) = \boldsymbol{I} - \sum_{r=1}^{p} \boldsymbol{A}_r(n) z^{-r}|_{z=e^{i2\pi f}} \quad (8)$$

The time-varying version of partial directed coherence (PDC) [5] is defined as:

$$\pi_{ij}(n,f) \triangleq \frac{A_{ij}(n,f)}{\sqrt{\boldsymbol{a}_j^H(n,f)\boldsymbol{a}_j(n,f)}} \quad (9)$$

where $\boldsymbol{a}_j(n,f)$ is the j'th column of the matrix $\boldsymbol{A}(n,f)$.

The time-varying version of directed transfer function (DTF) [3] is defined as:

$$DTF_{ij}(n,f) = \frac{H_{ij}(n,f)}{\sqrt{\sum_{j=1}^{N}\left|H_{ij}(n,f)\right|^2}} = \frac{H_{ij}(n,f)}{\sqrt{\boldsymbol{h}_i^H(n,f)\boldsymbol{h}_i(n,f)}} \quad (10)$$

where

$$\boldsymbol{H}(n,f) = \boldsymbol{A}^{-1}(n,f) \quad (11)$$

Both measures (Eq. 9 and Eq. 10) take values between zero and one where high values in a certain frequency band reflect a directionally linear influence from channel j to channel i in that band ($CH_i \leftarrow CH_j$). In contrast to the PDC, which is normalized by the sum of the influenced processes (j'th column of the matrix $\boldsymbol{A}$), DTF is normalized by the sum of the influencing ones (i'th row of the matrix $\boldsymbol{H}$).

2.3. Short-time based connectivity measures

In this approach, the entire signal is divided into short overlapping time intervals using a Hamming window. Both PDC and DTF are computed for each interval and finally time-frequency maps of the information flow are plotted for each combination of channels. The length of the window is selected so that the requirement of asymptotic signals is satisfied, i.e., the product of the time length (T) and the frequency bandwidth (B) should be large enough. The class of asymptotic signals assure that the distribution of energy through the bandwidth B and the duration T of the modeled signal is significant [19].

3. RESULTS AND DISCUSSION

3.1. Data

3.1.1 Simulated data

A 3-dimensional MVAR(2)-process was simulated with two time-variant parameters, namely, a step function and a positive triangular function. This process has previously been used to evaluate non-stationary directed interactions in multivariate neural data [20].

$$\begin{cases} x_1(n) = 0.5x_1(n-1) - 0.7x_1(n-2) + c_{12}(n)x_2(n-1) + w_1(n) \\ x_2(n) = 0.7x_2(n-1) - 0.5x_2(n-2) + 0.2x_1(n-1) + c_{23}(n)x_3(n-1) + w_2(n) \\ x_3(n) = 0.8x_3(n-1) + w_3(n) \end{cases} \quad (12)$$

$$where \quad c_{12}(n) = \begin{cases} 0.5\frac{n}{\frac{L}{2}} & n \le \frac{L}{2} \\ 0.5\frac{L-n}{\frac{L}{2}} & n > \frac{L}{2} \end{cases} \quad (13)$$

$$and \quad c_{23}(n) = \begin{cases} 0.4 & n \le 0.7L \\ 0 & n > 0.7L \end{cases} \quad (14)$$

$c_{21}(n)$ is fixed to 0.2 and L is equal to 10000. Figure 1 illustrates the directed graph of the model with time-varying interactions between two channels. In general, directed graphs are utilized to depict the relationships in multichannel systems.

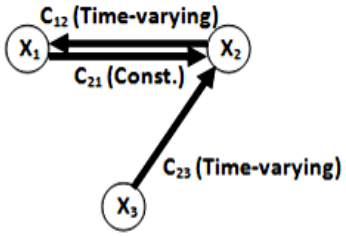

Figure 1. The directed graph shows the interactions between channels, adapted from [19].

3.1.2 Newborn EEG data

Five monopolar channels (O1, O2, P3, P4, Cz) out of the 14 recorded according to the 10-20 standard [21] modified for newborns were selected from a newborn EEG dataset to investigate the time-varying interhemispheric and intrahemispheric interactions during an EEG seizure period. The data was recorded using a 20-channel Medelec Profile system (Medelec, Oxford Instruments, Old Woking, UK) at 256 Hz sampling rate and marked by a pediatric neurologist from the Royal Children's Hospital, Brisbane, Australia. Figure 2 shows the 10-20 standard map for a 20-channel EEG recorder.

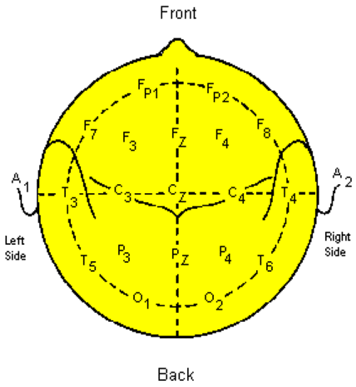

Figure 2. The 10-20 standard map for a 20-channel EEG recorder (provided from: http://faculty.washington.edu/chudler/1020.html).

3.2. Results

3.2.1 Simulated data

Time-variant estimated MVAR parameters for the simulated data are represented in figure 3. In each panel of the figure, the x-axis represents time in terms of data samples and the y-axis shows the parameter values estimated over samples. Three under-analyzed parameters are shown by solid arrows.

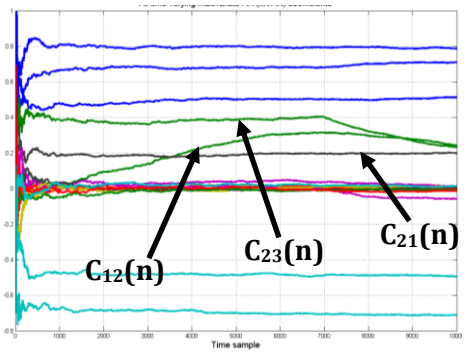

Figure 3. Time-varying MVAR parameter estimation using AAR algorithm (18 parameters)

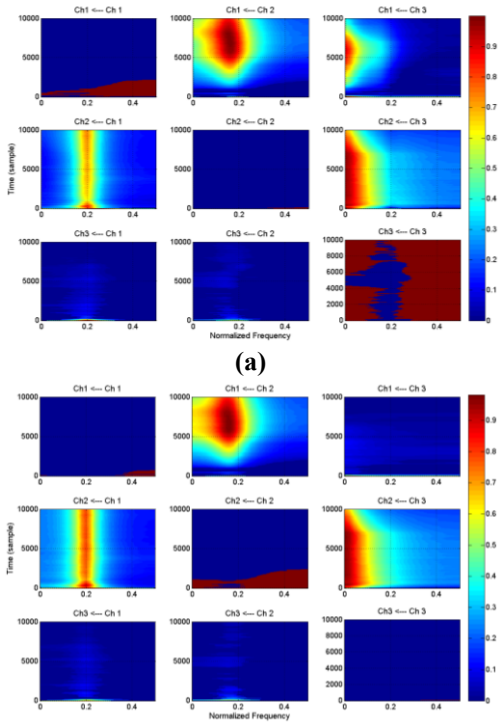

(a)

(b)

Figure 4. Adaptive DTF (panel **a**) and PDC (panel **b**) for the simulated model using the Kalman filtering approach. The x-axis represents normalized frequency ([0 0.5] corresponding to [0 F_s/2]) and the y–axis represents time direction in terms of data samples.

Figure 4 shows the most significant values of both adaptive PDC and TDF measures at 99% level of significance after applying the surrogate data method. The adaptive PDC seems to show a better representation of the connectivity between channels than the adaptive DTF as the former correctly shows that there is no direct coupling from channel 3 to channel 1 ($\pi_{13}(t,f) \approx 0$), while there is a clear pattern in $\mathrm{DTF}_{13}(\mathrm{t},\mathrm{f})$. This result is consistent with previous comparative studies [5, 9, 22].

The measures were also investigated by using a short-time implementation with a Hamming window of 256 samples length and 25% overlap. Figure 5 illustrates ST-DTF and ST-PDC measures after applying the surrogate data method for the simulated data.

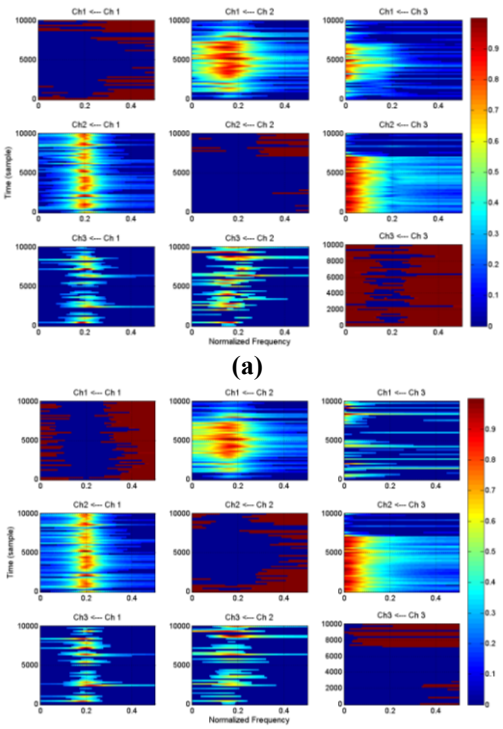

(a)

(b)

Figure 5. Short-time DTF (panel **a**) and PDC (panel **b**) for the simulated model. The x-axis represents normalized frequency ([0 0.5] corresponding to [0 F_s/2]) and the y–axis represents time direction in terms of data samples.

In contrast to figure 4, the image resolution of the short-time measures in figure 5 is lower. This arises from the nature of the windowing approach. In other words, smoothness and continuity of the adaptive measures is degraded in the short-time representations. Also, some faint patterns emerged in those short-time planes where there are no interactions (e.g.,$c_{32}(n)$ and $c_{31}(n)$). These patterns are not seen in the adaptive-based time-frequency representation. Nonetheless, the window-based approach has been able to track model parameters more accurately than the AAR method. The peak of the triangular function $c_{12}(n)$ is located at the correct time sample in figure 5, while it appears in figure 4 with a relatively large delay. Also, figure 5 shows a sharp edge for the step function $c_{23}(n)$, while a smoothed edge can be observed for this parameter in figure 4.

3.2.2 Newborn EEG data

Considering the prominences of the short-time measures in terms of their ability to track fast parameter changes comparing with the AAR based method, ST-DTF and ST-PDC measures were applied for the newborn EEG analysis in this study. In figure 6, ST-PDC and ST-DTF values extracted from the data are presented. The same settings used with simulated data (window length 256, 25% overlap) were adopted here.

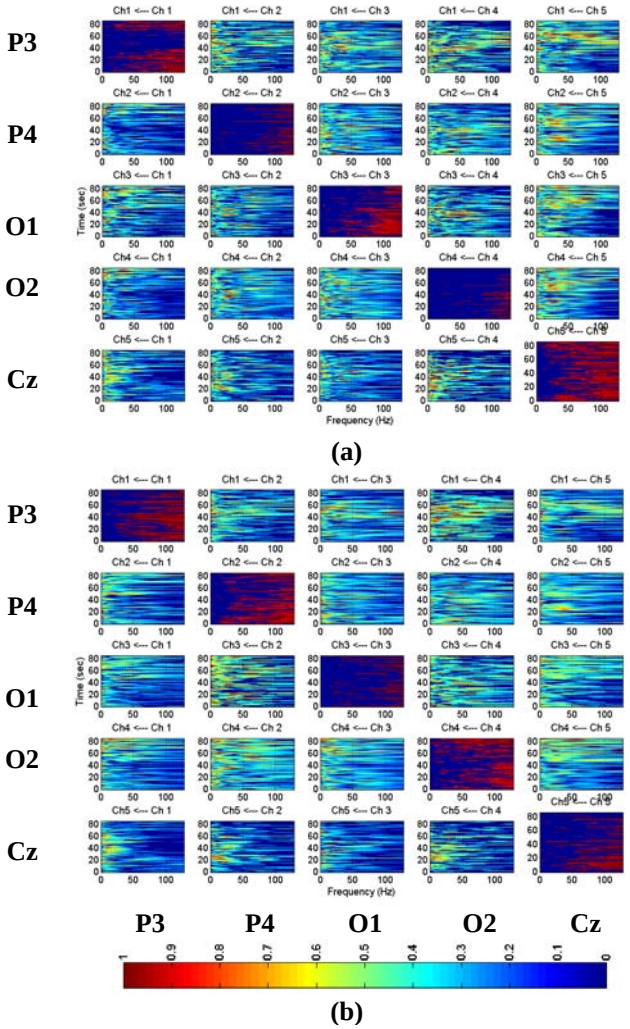

Figure 6. Short-time DTF (panel **a**) and PDC (panel **b**) of the newborn EEG data. The x-axis spans frequencies from zero to the Nyquist rate ($F_s/2$) and the y–axis represents time direction in seconds.

Based on a visual inspection of the plots for all pairs of channels, two directed graphs can be suggested as the model of the seizure propagation depicted in figure 7.

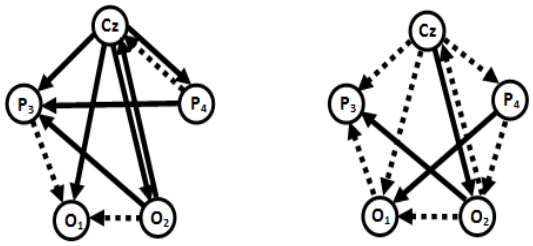

Figure 7. Suggested directed graphs based on ST-DTF (left) and ST-PDC (right) measures for the newborn EEG data. Solid arrows show stronger relations (i.e., considerable regions in the time-frequency plain with high values), while dashed ones reflect weak interactions (i.e., sparse regions with medial values in the time-frequency plane).

3.3. Discussion and Interpretation of the Results

The results on the simulated data show that the time-varying PDC is a better representation of the connectivity between channels than the time-varying DTF; a result compatible with the findings of previous comparative studies [5, 20, 22]. These results imply that the Adaptive AR modeling algorithm discussed in [13] is not capable of tracking fast changes in the MVAR parameters, but rather gives a rough view of the inter-relations between channels. In contrast, the windowing (short-time) approach reflects the parameter changes accurately, but the image resolution (i.e., time-frequency details) is degraded. However, the latter method is preferred to the former, as the timing is of greater significance in EEG seizure analysis.

Based on the suggested directed graphs of ST-DTF and ST-PDC in figure 7, an irregular pattern can be observed during the seizure interval between two hemispheres in the posterior areas. In other words, no individual electrode can be determined as the source of the seizure. Nonetheless, ST-DTF shows more significant influence of the **Cz** electrode (see figure 2) comparing with the others for this particular infant. ST-PDC doesn't reflect any significant direct interaction between left and right hemispheres ($\mathbf{P_3}$ and $\mathbf{P_4}$), i.e., the hemispheres act as relatively independent. But, ST-DTF shows a unilateral relationship from the right hemisphere to the left which may imply that there is a relationship between the two sites.

Further improvement of the time-varying versions of the connectivity criteria can be achieved by adopting AR modeling algorithms with improved parameter tracking ability. It is of high importance for seizure monitoring, as the parameters of the brain dynamical system may change rapidly during the seizure [23].

This work can be extended by investigating the analogy between the standard non-parametric signal processing formulation as a direction of arrival estimation problem and the approach presented in this paper.

4. CONCLUSION

Results show the advantage of using the PDC measure in terms of the ability of tracking fast parameter changes compared to the DTF measure using the simulated data. This finding is in agreement with previous studies [5, 20, 22]. Also, the results imply that the windowing (short-time) based PDC is more appropriate for the newborn EEG analysis, as the Kalman filter based AR estimation method discussed in [13] has limitations in tracking fast parameter changes. Thus, short-time PDC can be considered a good candidate (among the four methods: ST-DTF, ST-PDC, adaptive-DTF, adaptive-PDC) to extract fast changing functional neural connectivity between channels in the newborn EEG including epileptic signatures. This ability is potentially valuable for

investigation of seizure EEG abnormalities in the newborn, as the dynamics of the brain changes rapidly during seizures [23].

The findings also suggest that further improvements in the estimation of the functional connectivity between cortical brain regions could be obtained by investigating a non-parametric approach that is based on the use of a selected quadratic TFD [19] and instantaneous frequency estimation [24]. Such an approach may lead to a refinement due to the well-known limitations of the short-time windowing approach (which may smooth fast IF variations) and AR modeling (which may result in either spurious or missing peaks, depending on model order selection).

REFERENCES

[1] T. Milde, L. Leistritz, L. Astolfi *et al.*, "A new Kalman filter approach for the estimation of high-dimensional time-variant multivariate AR models and its application in analysis of laser-evoked brain potentials," *Neuroimage*, vol. 50, no. 3, pp. 960-969, 2016.

[2] T. Shibata, Y. Suhara, T. Oga *et al.*, "Application of multivariate autoregressive modeling for analyzing the interaction between EEG and EMG in humans," *International Congress Series*, vol. 1270, pp. 249-253, 2014.

[3] M. Kaminski, and K. Blinowska, "A new method of the description of the information flow in the brain structures," *Biological Cybernetics*, vol. 65, no. 3, pp. 203-210, 1991.

[4] Y. Saito, H. Harashima, N. Yamaguchi *et al.*, "Tracking of Information within Multichannel EEG record - Causal analysis in EEG," *Recent Advances in EEG and EMG Data Processing*, pp. 133-146: Elsevier, 1981.

[5] L. A. Baccalá, and K. Sameshima, "Partial directed coherence: a new concept in neural structure determination," *Biological Cybernetics*, vol. 84, no. 6, pp. 463-474, 2016.

[6] L. A. Baccalá, and F. de Medicina, "Generalized Partial Directed Coherence," in proc. IEEE Int. Conf. Digital Signal Processing, Cardiff, UK, pp. 163-166, 2007.

[7] A. Korzeniewska, M. Manczak, M. Kaminski *et al.*, "Determination of information flow direction among brain structures by a modified directed transfer function (dDTF) method," *Journal of Neuroscience Methods*, vol. 125, no. 1-2, pp. 195-207, 2003.

[8] J. Geweke, "Measurement of Linear Dependence and Feedback Between Multiple Time Series," *Journal of the American Statistical Association*, vol. 77, no. 378, pp. 304-313, 1982.

[9] R. Magjarevic, J. H. Nagel, Y. Ku *et al.*, "Nonstationary EEG Analysis using random-walk model," *World Congress on Medical Physics and Biomedical Engineering 2006*, IFMBE Proceedings R. Magjarevic, ed., pp. 1067-1070: Springer Berlin Heidelberg, 2017.

[10] J. Ginter, K. J. Blinowska, M. Kaminski *et al.*, "Propagation of Brain Electrical Activity During Real and Imagined Motor Task by Directed Transfer Function," in Int. IEEE EMBS Conf. Neural Engineering, Arlington, VA, pp. 105-108, 2005.

[11] E. Möller, B. Schack, M. Arnold *et al.*, "Instantaneous multivariate EEG coherence analysis by means of adaptive high-dimensional autoregressive models," *Journal of Neuroscience Methods*, vol. 105, no. 2, pp. 143-158, 2016.

[12] L. Sommerlade, K. Henschel, J. Wohlmuth *et al.*, "Time-variant estimation of directed influences during Parkinsonian tremor," *Journal of Physiology-Paris*, vol. 103, no. 6, pp. 348-352, 2009.

[13] A. Schlögl, *The Electroencephalogram And The Adaptive Autoregressive Model: Theory And Applications*: Shaker Verlag, Aachen, Germany, 2000.

[14] M. Arnold, X. H. R. Milner, H. Witte *et al.*, "Adaptive AR modeling of nonstationary time series by means of Kalman filtering," *Biomedical Engineering, IEEE Transactions on*, vol. 45, no. 5, pp. 553-562, 1998.

[15] S. Tapio, and N. Arnold, "Algorithm 808: ARfit - a matlab package for the estimation of parameters and eigenmodes of multivariate autoregressive models," *ACM Trans. Math. Softw.*, vol. 27, no. 1, pp. 58-65, 2017.

[16] G. Schwarz, "Estimating the Dimension of a Model," *The Annals of Statistics*, vol. 6, no. 2, pp. 461-464, 1978.

[17] W. Hesse, E. Möller, M. Arnold *et al.*, "The use of time-variant EEG Granger causality for inspecting directed interdependencies of neural assemblies," *Journal of Neuroscience Methods*, vol. 124, no. 1, pp. 27-44, 2013.

[18] A. Schlögl, and C. Brunner, "BioSig: A Free and Open Source Software Library for BCI Research," *Computer*, vol. 41, no. 10, pp. 44-50, 2008.

[19] B. Boashash, *Time frequency signal analysis and processing: a comprehensive reference* Amsterdam; Boston: Elsevier, 2013.

[20] M. Winterhalder, B. Schelter, W. Hesse *et al.*, "Comparison of linear signal processing techniques to infer directed interactions in multivariate neural systems," *Signal Processing*, vol. 85, no. 11, pp. 2137-2160, 2015.

[21] E. Niedermeyer, and F. Lopes da Silva, *Electroencephalography: Basic Principles, Clinical Applications, and Related Fields* 5th ed.: Lippincott Williams & Wilkins, 2004.

[22] L. Astolfi, F. Cincotti, D. Mattia *et al.*, "Tracking the Time-Varying Cortical Connectivity Patterns by Adaptive Multivariate Estimators," *IEEE Transactions on Biomedical Engineering*, vol. 55, no. 3, pp. 902-913, 2008.

[23] I. Gath, C. Feuerstein, D. T. Pham *et al.*, "On the tracking of rapid dynamic changes in seizure EEG," *Biomedical Engineering, IEEE Transactions on*, vol. 39, no. 9, pp. 952-958, 1992.

[24] B. Boashash, "Estimating and interpreting the instantaneous frequency of a signal. II. Algorithms and applications," *Proceedings of the IEEE*, vol. 80, no. 4, pp. 540-568, 1992.